Journal of Computational Applied Mechanics 2025, 56(2): 345-363

DOI: 10.22059/jcamech.2025.391218.1390

RESEARCH PAPER

Nonlocal Magneto-Thermoelastic Interactions in a Thin Slim Strip Due to a Moving Heat Source Via a Refined Lord–Shulman Theory

Maryam H. Aljadani [a], Hamada F. El-Mekawy [b], Zahra S. Hafed [c], Ashraf M. Zenkour [d,e*]

[a] *Department of Mathematics, Jamoum University College, Umm Al-Qura University, Makkah 21421, Saudi Arabia*

[b] *Department of Management Information Systems, College of Business and Economics, Qassim University, Buraidah 51452, P.O. Box 6666, Saudi Arabia*

[c] *Department of Mathematics, Faculty of Science, King Khalid University, Abha, 21589, Saudi Arabia*

[d] *Department of Mathematics, Faculty of Science, King Abdulaziz University, Jeddah 21589, Saudi Arabia*

[e] *Department of Mathematics, Faculty of Science, Kafrelsheikh University, Kafrelsheikh 33516, Egypt*

Abstract

In this article, a new nonlocal model of the heat equation based on Eringen's nonlocal elasticity and Lord–Shulman one relaxation time is introduced. The thermoelastic communications in an isotropic, homogeneous thin slim strip under a traveling heat source and placed in a magnetic field are studied. The Laplace transform technique is adopted to get the transform domain solution in a closed form. The outcomes of all variables are determined in the Laplace domain and then they are transferred to the physical domain by employing its fast inversion technique. The impacts of the nonlocal index and applied magnetic field in addition to the speed of the heat source parameter on the quantities are discussed in detail. The current analysis is believed to be beneficial for the theoretical formulation of thermoelastic analyses at the nanoscale, and the outcomes are useful to the practical design of nanosized configurations in thermal environments.

Keywords: Nonlocal thermoelasticity; thin slim strip; moving heat source; magnetic field; LS theory.

1. Introduction

The nonlocal theory of elasticity is applied to explore nanomechanics efforts. In the very first years, the models of the nonlocal beams (rods, thin strips) demanded an increasing amount of attention. Eringen [1, 2] and Eringen and Edelen [3] established the nonlocal continuum mechanics theory to address issues with nanostructures at a microscopic scale. The investigators in what follows, have used the nonlocal theory of thermoelasticity [4-19] in their investigations.

Recently, Sarkar [20] examined the transient responses of a finite-length thermoelastic rod exposed to a moving source of heat using Eringen's nonlocal elasticity theory along with the thermoelasticity theory introduced by Lord and Shulman. Nonlocal elasticity theory was used by Zarezadeh et al. [21] to investigate the impact of nonlocal magneto-thermoelastic responses on FG nano-rod. In the context of the Lord-Shulman (LS) and thermoelasticity theory of three-phase-lag according to Eringen's nonlocal elasticity, Mondal [22] and Bayones et al. [23] studied the

* Corresponding author.

E-mail address: zenkour@kau.edu.sa

transient phenomena resulting from the impact of a moving heat source and a magnetic field within a rod. Abouelregal [24] discussed the size-dependent behavior of a finite thermoelastic rod influenced by a moving heat source using Eringen's nonlocal elasticity theory. In the framework of a three-phase-lag heat conduction model, Satish et al. [25] investigated the thermoelastic damping of a longitudinally vibrating nanorod at a small scale using Eringen's nonlocal elasticity theory.

Various applications have been considered for the thermoelastic responses of thin slim strips in the literature. He and Cao [26] used the LS theory to talk about the magneto-thermoelastic model of a narrow, slim strip subjected to a moving source of heat and placed in a magnetic field. Abbas [27] addressed the issue of narrow, slender strips using the Green and Lindsay hypothesis of two temperatures. A problem of transient response for a thin strip with one end sensitive to thermal and chemical disturbances was addressed by Li et al. [28]. Abo-Dahab et al. [29] examined the thermoelastic response of an FG thin slim strip based on the LS theory.

All investigations concerning the thermoelastic responses of thin slim strips are considered in the classical (local) theory of elasticity. In this research work, within the framework of Eringen's nonlocal theory, a finite thin slim strip magneto-thermoelastic dynamic behavior is investigated. The strip is placed in an external magnetic field, fixed at both endpoints, and subjected to a moving heat supply. The Laplace technique has been adopted to introduce and solve thermoelastic coupled equations. The distributions of temperature, displacement, dilatation, and stress along the axial direction are studied in both cases of local and nonlocal elasticity. The impacts of the velocity of the applied magnetic field, nonlocal parameter, and the moving source of heat on all variables are investigated.

2. Nonlocal Thermoelasticity Theory

Corresponding to the nonlocal elasticity theory by Eringen [1-3], the nonlocal stress components $\tilde{\tau}(\vec{x})$ at any point $\vec{x}$ in a solid can be stated as

$$\tilde{\tau}(\vec{x}) = \int_V \chi(|\vec{x}-\vec{x}'|,\xi)\,\tilde{\sigma}(\vec{x}')\mathrm{d}V(\vec{x}'), \tag{1}$$

where $\tilde{\sigma}(\vec{x}')$ represent the classical local stress components at two neighboring points $\vec{x}'$ and $\vec{x}$, $|\vec{x}-\vec{x}'|$ is the Euclidean space, V is the elastic body volume, and the function χ represents a nonlocal Kernel indicating the impact of distant communications of material points between $\vec{x}$ and $\vec{x}'$. Moreover, ξ represents a material elastic nonlocal parameter provided by $\xi = e_0 a/l$, which differs on inner a and outer characteristic lengths l by modifying constant e_0, contingent on each material. ξ is a typical length that involves the microstructure evidence associated with the discreteness of the material.

Considering that the material of the slim strip is isotropic, then the classical stress components $\tilde{\sigma}(\vec{x}')$ associated with temperature θ is given by the following Neumann-Duhamel law:

$$\tilde{\sigma}(\vec{x}') = 2\mu\,\tilde{\varepsilon}(\vec{x}') + [\lambda(\nabla\cdot\vec{u}) - \gamma\theta]\tilde{I}, \tag{2}$$

where $\vec{I}$ is the identity tensor, $\tilde{\varepsilon}(\vec{x}')$ represents the tensor of a classical local strain and $\vec{u}(\vec{x}')$ denote a reference point $\vec{x}'$ displacement vector in the medium. The linear Cauchy's infinitesimal strain relations are given by

$$\tilde{\varepsilon}(\vec{x}') = \frac{1}{2}[\nabla\vec{u} + \nabla(\vec{u}^T)]. \tag{3}$$

All field quantities are, in general, functions of $(\vec{x},t)$, the direct vector/tensor notation is employed, $\theta = T - T_0$ is the difference in temperature where T and T_0 denote the current and reference temperatures of the slim strip in its natural state expected to be such that $|\theta/T_0| \ll 1$, $\gamma = (3\lambda+2\mu)\alpha_t$, α_t is the linear expansion coefficient, λ and μ being Lamé's constants.

The constitutive equations of gradient type for a suitable form of the nonlocal kernel can be represented by

$$(1-\xi^2\nabla^2)\tilde{\tau}(\vec{x}) = \tilde{\sigma}(\vec{x}'), \tag{4}$$

which considers the impact of size on a nanostructure's response.

The following equations of motion are produced by the balance of linear momentum

$$\nabla\cdot\tilde{\tau} + \vec{F} = \rho\frac{\partial^2\vec{u}}{\partial t^2}, \tag{5}$$

where $\vec{F}$ denotes the vector of outer body force and ρ denotes the material density. Once applying Equation (4), the linear momentum balance, Equation (5), outcomes in the resulting equation of motion

$$\nabla\cdot\tilde{\sigma} + (1-\xi^2\nabla^2)\vec{F} = \rho(1-\xi^2\nabla^2)\frac{\partial^2\vec{u}}{\partial t^2}, \tag{6}$$

It should be noted that the nonlocal displacement field of a structure exposed to an outward body force field $\vec{F}$ and an inertial body force $-\rho\frac{\partial^2\vec{u}}{\partial t^2}$ is identical to that of a classical structure exposed to the force of exterior $(1-\xi^2\nabla^2)\vec{F}$ and the force of inertial body $-\rho(1-\xi^2\nabla^2)\frac{\partial^2\vec{u}}{\partial t^2}$. In the context of the temperature and displacement, the dynamic equations can be obtained as

$$(\lambda+\mu)\nabla(\nabla\vec{u})+\mu\nabla^2\vec{u}-\gamma\nabla\theta+(1-\xi^2\nabla^2)\vec{F}=\rho(1-\xi^2\nabla^2)\frac{\partial^2\vec{u}}{\partial t^2}. \tag{7}$$

When the internal characteristic length is disregarded, or when one assumes that a medium's particles are constantly dispersed, it is possible to conclude that $\xi=0$, and Equation (4) becomes the classical local thermoelasticity constitutive equation. The classical law of Fourier, which connects the vector of heat flux $\vec{q}$ to the temperature gradient as follows, forms the foundation of the classical theory of heat conductivity, upon which classical thermoelasticity is built:

$$\vec{q}=-K\nabla\theta, \tag{8}$$

where K denotes the thermal conductivity. The heat conduction equation is provided by

$$\rho c_v\frac{\partial\theta}{\partial t}+\gamma T_0\frac{\partial}{\partial t}(\nabla\cdot\vec{u})=-\nabla\cdot\vec{q}+Q, \tag{9}$$

where c_v is the specific heat at constant deformation and Q is the external heat source.

Modified Fourier's law of heat transfer was demonstrated as [30-35]

$$\left(1+\sum_{n=1}^{N}\frac{t_0^n}{n!}\frac{\partial^n}{\partial t^n}\right)\vec{q}=-K\nabla\theta, \tag{10}$$

where t_0 represents the first relaxation time presented by Lord and Shulman. Taking the divergence of the sides of Equation (6) and using Equation (10), one obtains the equation of a refined generalized heat conduction extended by Lord and Shulman [36, 37] as

$$K\nabla^2\theta=\left(1+\sum_{n=1}^{N}\frac{t_0^n}{n!}\frac{\partial^n}{\partial t^n}\right)\left[\rho c_v\frac{\partial\theta}{\partial t}+\gamma T_0\frac{\partial}{\partial t}(\nabla\cdot\vec{u})-Q\right]. \tag{11}$$

In the above refined Lord and Shulman (LS) theory N can be 5 or more. However, the simple LS theory is considered to correspond to the value of $N=1$ as [13]

$$K\nabla^2\theta=\left(1+t_0\frac{\partial}{\partial t}\right)\left[\rho c_v\frac{\partial\theta}{\partial t}+\gamma T_0\frac{\partial}{\partial t}(\nabla\cdot\vec{u})-Q\right]. \tag{12}$$

However, for $t_0=0$ we obtain the classical thermoelasticity theory [38]

$$K\nabla^2\theta=\rho c_v\frac{\partial\theta}{\partial t}+\gamma T_0\frac{\partial}{\partial t}(\nabla\cdot\vec{u})-Q. \tag{13}$$

The above system of equations describes the nonlocal thermoelasticity model. It can be noticed that the equivalent local thermoelasticity model is found by setting $\xi=0$ in all equations.

The charge density is ignored in the following formulation of electromagnetic equations of Maxwell's for an electrically conducting, homogenous thermoelastic model:

$$\begin{aligned}&\nabla\times\vec{E}=-\mu_0\frac{\partial\vec{h}}{\partial t},\quad \vec{J}=\sigma_0\left(\vec{E}+\frac{\partial\vec{u}}{\partial t}\times\vec{B}\right),\\&\vec{h}=\nabla\times\left(\vec{u}\times\vec{H}\right),\quad \nabla\cdot\vec{h}=0,\quad \vec{B}=\mu_0\vec{H},\end{aligned} \tag{14}$$

where μ_0 donates the magnetic permeability, σ_0 donates the electric conductivity, $\vec{H}$ donates a magnetic field, $\vec{J}$ donates a current density, $\vec{h}$ is the generated magnetic field and $\vec{E}$ is the generated electric field.

3. Formulation of the Problem

The present study concerns the matter of an isotropic and homogeneous thermoelastic thin strip, which is initially devoid of any strain or stress but exhibits a uniform temperature distribution T_0. Considering the x-axis is the axial direction of the strip. The axial direction of the strip will be represented by the x -axis. The location of the moving source of heat $Q(x,t)$ and its propagation along the x direction is defined by the plane area $x=0$. The dynamic issue associated with a thin, slim strip can be examined as a problem that is one-dimensional in the structure, with all physical variables being dependent entirely on the space variable x and the time parameter t. The strip is affixed at both endpoints and exposed to a moving heat source plane that travels along the direction of the x-axis.

According to one-dimensional problems, the displacement field is simplified to a certain extent

$$u_x = u(x,t), \quad u_y = u_z = 0. \tag{15}$$

A magnetic field acting perpendicular to the strip's axial direction with a constant strength $\vec{H} \equiv (0, H_x, 0)$. The total field $\vec{E}$ disappears uniformly in the medium interior because there is no applied external electric field. The vector elements of electromagnetic induction are:

$$B_x = B_z = 0, \quad B_y = \mu_0 H_x, \tag{16}$$

while the Lorentz force $\vec{F} = \vec{J} \times \vec{B}$ caused by utilizing a longitudinal magnetic field $\vec{H}$ acting in Equation (7) is stated as

$$F_x = -\sigma_0 \mu_0^2 H_x^2 \frac{\partial u}{\partial t}, \quad F_y = F_z = 0. \tag{17}$$

Equation (7) also reduces the stress tensor to

$$\left(1 - \xi^2 \frac{\partial^2}{\partial x^2}\right) \tau = \sigma = (\lambda + 2\mu) \frac{\partial u}{\partial x} - \gamma \theta. \tag{18}$$

With the aid of Equations (7), (15), and (16), we attain the dynamic equation for the one-dimensional as

$$\rho \left(1 - \xi^2 \frac{\partial^2}{\partial x^2}\right) \frac{\partial^2 u}{\partial t^2} = (\lambda + 2\mu) \frac{\partial^2 u}{\partial x^2} - \gamma \frac{\partial \theta}{\partial x} - \sigma_0 \mu_0^2 H_x^2 \left(1 - \xi^2 \frac{\partial^2}{\partial x^2}\right) \frac{\partial u}{\partial t}. \tag{19}$$

The heat conduction equation (11) is now provided by

$$K \frac{\partial^2 \theta}{\partial x^2} = \left(1 + \sum_{n=1}^{N} \frac{\tau_0^n}{n!} \frac{\partial^n}{\partial t^n}\right) \left[\rho c_v \frac{\partial \theta}{\partial t} + \gamma T_0 \frac{\partial}{\partial t}\left(\frac{\partial u}{\partial x}\right) - Q\right]. \tag{20}$$

The dimensionless quantities presented below are being considered

$$\begin{gathered} \{x', u', \xi'\} = c_0 \eta_0 \{x, u, \xi\}, \quad \{t', \tau_1'\} = c_0^2 \eta_0 \{t, \tau_1\}, \quad \theta' = \frac{\theta}{T_0}, \\ \sigma' = \frac{\sigma}{\lambda + 2\mu}, \quad \tau' = \frac{\tau}{\lambda + 2\mu}, \quad Q' = \frac{Q}{K T_0 c_0^2 \eta_0^2}, \quad c_0^2 = \frac{\lambda + 2\mu}{\rho}, \quad \eta_0 = \frac{\rho c_v}{K}. \end{gathered} \tag{21}$$

The governing equations, denoted as (18) to (20), can be expressed as follows by removing the primes:

$$\left(1 - \xi^2 \frac{\partial^2}{\partial x^2}\right) \tau = \sigma = \frac{\partial u}{\partial x} - \eta_1 \theta, \tag{22}$$

$$\left(1 - \xi^2 \frac{\partial^2}{\partial x^2}\right) \frac{\partial^2 u}{\partial t^2} = \frac{\partial^2 u}{\partial x^2} - \eta_1 \frac{\partial \theta}{\partial x} - \epsilon \left(1 - \xi^2 \frac{\partial^2}{\partial x^2}\right) \frac{\partial u}{\partial t}, \tag{23}$$

$$\frac{\partial^2 \theta}{\partial x^2} = \left(1 + \sum_{n=1}^{N} \frac{\tau_0^n}{n!} \frac{\partial^n}{\partial t^n}\right) \left[\frac{\partial \theta}{\partial t} + \eta_2 \frac{\partial}{\partial t}\left(\frac{\partial u}{\partial x}\right) - Q\right], \tag{24}$$

where

$$\eta_1 = \frac{\gamma T_0}{\rho c_0^2}, \quad \epsilon = \frac{\sigma_0 \mu_0^2 H_x^2}{\rho c_0^2 \eta_0}, \quad \eta_2 = \frac{\gamma}{K \eta_0}. \tag{25}$$

The above-governing equations start the local formulation if the nonlocal parameter ξ is assigned a value of zero. The objective of the present study is to define the temperature, displacement, and nonlocal thermal stress of the slim strip described in Equations (22)–(24).

4. Initial and Boundary Conditions

The homogeneous initial conditions are shown as

$$\theta(x,0) = \left.\frac{\partial^n \theta}{\partial t^n}\right|_{t=0} = 0 = u(x,0) = \left.\frac{\partial^n u}{\partial t^n}\right|_{t=0}, \quad n = 1, \dots, N. \tag{26}$$

Also, assuming that both endpoints of the strip are fixed i.e.

$$u(0,t) = u(L,t) = 0, \tag{27}$$

where L is the dimensionless length of the strip.

Also, we consider the two ends to be heat insulation, the boundary should satisfy the following relation

$$u(0,t) = u(L,t) = 0, \tag{28}$$

$$\frac{\partial \theta}{\partial x} = 0 \quad \text{on} \quad x = 0, L. \tag{29}$$

The strip is under a moving source of heat with fixed intensity Q_0 that constantly releases energy while traveling with a fixed speed ϑ along the positive x-axis. The next dimensionless structure is thought to represent this moving source of heat [26].

$$Q = Q_0 \delta(x - \vartheta t) \quad \text{on} \quad x = 0, L. \tag{30}$$

5. Resolution of the Laplace Transform Domain Issue

The utilization of the Laplace transform method can result in the finding of the solution in a closed form for the governing and constitutive equations. Applying the following Laplace transform

$$\bar{f}(x,s) = \int_0^\infty f(x,t) \mathrm{e}^{-st} \mathrm{d}t, \tag{31}$$

to Equations (22)–(24) on both sides and utilizing the homogeneous initial conditions presented in Equation (24), the field equations in the Laplace transform domain can be derived as follows

$$\left(1 - \xi^2 \frac{\mathrm{d}^2}{\mathrm{d}x^2}\right) \bar{\tau} = \bar{\sigma} = \frac{\mathrm{d}\bar{u}}{\mathrm{d}x} - \eta_1 \bar{\theta}, \tag{32}$$

$$\left(\frac{\mathrm{d}^2}{\mathrm{d}x^2} - \eta_3\right) \bar{u} - \eta_4 \frac{\mathrm{d}\bar{\theta}}{\mathrm{d}x} = 0, \tag{33}$$

$$\left(\frac{\mathrm{d}^2}{\mathrm{d}x^2} - \eta_5\right) \bar{\theta} - \eta_6 \frac{\mathrm{d}\bar{u}}{\mathrm{d}x} = -Q_1 \mathrm{e}^{-(s/\vartheta)x}, \tag{34}$$

where

$$\begin{gathered} Q_1 = \frac{\varpi Q_0}{\vartheta}, \quad \eta_3 = \frac{s(\epsilon+s)}{\xi^2 s(\epsilon+s)+1}, \quad \eta_4 = \frac{\eta_1}{\xi^2 s(\epsilon+s)+1}, \\ \eta_5 = \varpi s, \quad \eta_6 = \eta_2 \eta_5, \quad \varpi = 1 + \sum_{n=1}^{N} \frac{t_0^n}{n!} s^n. \end{gathered} \tag{35}$$

Elimination $\bar{\theta}$ or $\bar{u}$ from Equations (33) and (34), one obtains:

$$\left(\frac{\mathrm{d}^4}{\mathrm{d}x^4} - 2c_1 \frac{\mathrm{d}^2}{\mathrm{d}x^2} + c_2\right) \bar{u}(x) = c_3 \mathrm{e}^{-(s/\vartheta)x}, \tag{36}$$

$$\left(\frac{\mathrm{d}^4}{\mathrm{d}x^4} - 2c_1 \frac{\mathrm{d}^2}{\mathrm{d}x^2} + c_2\right) \bar{\theta}(x) = c_4 \mathrm{e}^{-(s/\vartheta)x}, \tag{37}$$

where the coefficients c_1, c_2, c_3 and c_4 are given by

$$c_1 = \frac{1}{2}(\eta_3 + \eta_5 + \eta_4 \eta_6), \quad c_2 = \eta_3 \eta_5, \quad c_3 = \frac{\eta_4 Q_1 s}{\vartheta}, \quad c_4 = \left(\eta_3 - \frac{s^2}{\vartheta^2}\right) Q_1. \tag{38}$$

The solutions of Equations (36) and (37) can be represented as

$$\bar{u}(x) = \sum_{n=1}^{2} \left(A_n \mathrm{e}^{\zeta_n x} + B_n \mathrm{e}^{-\zeta_n x}\right) + \bar{c}_3 \mathrm{e}^{-\zeta_3 x}, \tag{39}$$

$$\bar{\theta}(x) = \sum_{n=1}^{2} \beta_n \left(A_n \mathrm{e}^{\zeta_n x} - B_n \mathrm{e}^{-\zeta_n x}\right) - \beta_3 \bar{c}_3 \mathrm{e}^{-\zeta_3 x}, \tag{40}$$

where A_n and B_n, $(n = 1,2)$ are two integral constants subject to s to be obtained from the boundary conditions, while β_j and $\bar{c}_3$ are represented as

$$\beta_j = \frac{\zeta_j^2 - \eta_3}{\zeta_j \eta_4}, \quad \bar{c}_3 = \frac{c_3}{\zeta_3^4 - 2c_1 \zeta_3^2 + c_2}, \quad \zeta_3 = \frac{s}{\vartheta}, \quad j = 1,2,3. \tag{41}$$

In Equations (39) and (40), ζ_1 and ζ_2 are the roots of the individual equation

$$\zeta^4 - 2c_1\zeta^2 + c_2 = 0, \tag{42}$$

and they are given by

$$\zeta_1^2, \zeta_2^2 = c_1 \mp \sqrt{c_1^2 - c_2}. \tag{43}$$

The component of stress $\bar{\tau}$ may be calculated using Equations (39) and (40) in Equation (32) as

$$\left(1 - \xi^2 \frac{\mathrm{d}^2}{\mathrm{d}x^2}\right)\bar{\tau} = \bar{\sigma} = \sum_{n=1}^{2} \bar{\beta}_n\left(A_n \mathrm{e}^{\zeta_n x} - B_n \mathrm{e}^{-\zeta_n x}\right) - \bar{\beta}_3 \bar{c}_3 \mathrm{e}^{-\zeta_3 x}, \tag{44}$$

where

$$\bar{\beta}_j = \zeta_j - \beta_j \eta_1, \quad j = 1,2,3. \tag{45}$$

The classical local stress $\bar{\sigma}$ in Equation (44) is easily given while the nonlocal stress $\bar{\tau}$ is given by solving Equation (44) in the form

$$\bar{\tau} = \sum_{n=1}^{2} \hat{\beta}_n\left(A_n \mathrm{e}^{\zeta_n x} - B_n \mathrm{e}^{-\zeta_n x}\right) - \hat{\beta}_3 \bar{c}_3 \mathrm{e}^{-\zeta_3 x} + A_4 \mathrm{e}^{\zeta_4 x} + B_4 \mathrm{e}^{-\zeta_4 x}, \tag{46}$$

where A_4 and B_4 are additional integral constants and

$$\hat{\beta}_j = \frac{\bar{\beta}_j \zeta_4^2}{\zeta_4^2 - \zeta_j^2}, \quad \zeta_4 = \frac{1}{\xi}, \quad j = 1,2,3. \tag{47}$$

After utilizing Laplace transform in Equations (28) and (29), the boundary conditions take the forms

$$\bar{u} = \frac{\mathrm{d}\bar{\theta}}{\mathrm{d}x} = 0 \quad \text{at} \quad \bar{x} = 0,1, \quad \bar{x} = x/L. \tag{48}$$

Substituting Equations (39) and (40) into the above boundary conditions, one attains

$$\begin{bmatrix} 1 & 1 & 1 & 1 \\ \mathrm{e}^{\zeta_1} & \mathrm{e}^{-\zeta_1} & \mathrm{e}^{\zeta_2} & \mathrm{e}^{-\zeta_2} \\ \beta_1\zeta_1 & \beta_1\zeta_1 & \beta_2\zeta_2 & \beta_2\zeta_2 \\ \beta_1\zeta_1\mathrm{e}^{\zeta_1} & \beta_1\zeta_1\mathrm{e}^{-\zeta_1} & \beta_2\zeta_2\mathrm{e}^{\zeta_2} & \beta_2\zeta_2\mathrm{e}^{-\zeta_2} \end{bmatrix} \begin{Bmatrix} A_1 \\ B_1 \\ A_2 \\ B_2 \end{Bmatrix} = -\bar{c}_3 \begin{Bmatrix} 1 \\ \mathrm{e}^{-\zeta_3} \\ \beta_3\zeta_3 \\ \beta_3\zeta_3\mathrm{e}^{-\zeta_3} \end{Bmatrix}. \tag{49}$$

After solving the above system we get the unknown parameters A_n, B_n in the form

$$\begin{aligned} A_1 &= \frac{\bar{c}_3(\beta_3\zeta_3 - \beta_2\zeta_2)(\mathrm{e}^{-\zeta_1} - \mathrm{e}^{-\zeta_3})}{(\beta_1\zeta_1 - \beta_2\zeta_2)(\mathrm{e}^{\zeta_1} - \mathrm{e}^{-\zeta_1})}, \quad B_1 = -\frac{\bar{c}_3(\beta_3\zeta_3 - \beta_2\zeta_2)(\mathrm{e}^{\zeta_1} - \mathrm{e}^{-\zeta_3})}{(\beta_1\zeta_1 - \beta_2\zeta_2)(\mathrm{e}^{\zeta_1} - \mathrm{e}^{-\zeta_1})}, \\ A_2 &= \frac{\bar{c}_3(\beta_1\zeta_1 - \beta_3\zeta_3)(\mathrm{e}^{-\zeta_2} - \mathrm{e}^{-\zeta_3})}{(\beta_1\zeta_1 - \beta_2\zeta_2)(\mathrm{e}^{\zeta_2} - \mathrm{e}^{-\zeta_2})}, \quad B_2 = -\frac{\bar{c}_3(\beta_1\zeta_1 - \beta_3\zeta_3)(\mathrm{e}^{\zeta_2} - \mathrm{e}^{-\zeta_3})}{(\beta_1\zeta_1 - \beta_2\zeta_2)(\mathrm{e}^{\zeta_2} - \mathrm{e}^{-\zeta_2})}. \end{aligned} \tag{50}$$

The nonlocal impact has recently been recognized as an important consideration that could not be neglected when determining stress. So, to get the complete form of the nonlocal stress $\bar{\tau}$ we need to add two boundary conditions in the form

$$\bar{\tau} = 0 \quad \text{at} \quad \bar{x} = 0,\, 1, \tag{51}$$

and using Equation (46) to get

$$\begin{aligned} A_4 &= \frac{1}{\mathrm{e}^{\zeta_4} - \mathrm{e}^{-\zeta_4}}\left\{\sum_{n=1}^{2} \hat{\beta}_n\left[A_n\left(\mathrm{e}^{-\zeta_4} - \mathrm{e}^{\zeta_n}\right) - B_n\left(\mathrm{e}^{-\zeta_4} - \mathrm{e}^{-\zeta_n}\right)\right] - \hat{\beta}_3\bar{c}_3\left(\mathrm{e}^{-\zeta_4} - \mathrm{e}^{-\zeta_3}\right)\right\}, \\ B_4 &= -\frac{1}{\mathrm{e}^{\zeta_4} - \mathrm{e}^{-\zeta_4}}\left\{\sum_{n=1}^{2} \hat{\beta}_n\left[A_n\left(\mathrm{e}^{\zeta_4} - \mathrm{e}^{\zeta_n}\right) - B_n\left(\mathrm{e}^{\zeta_4} - \mathrm{e}^{-\zeta_n}\right)\right] - \hat{\beta}_3\bar{c}_3\left(\mathrm{e}^{\zeta_4} - \mathrm{e}^{-\zeta_3}\right)\right\}. \end{aligned} \tag{52}$$

To determine the studied fields (θ^*, u^*, e^*, σ^*, and τ^*) in the physical domain, the numerical findings are obtained using the Riemann-sum approximation approach. One can read about these techniques in detail in Honig and Hirdes [39].

6. Local thermoelasticity theory

To obtain the local expression, set the nonlocal parameter ξ to zero in the governing equations given above. The purpose of the current investigation is to examine the thin strip defined by Equations (22)-(24) in terms of displacement, temperature, and nonlocal thermal stress along its axial direction.

The dimensionless governing equations for the coupled and refined thermoelasticity theories of the thin slim strip may be finally written as

$$\tau = \sigma = \frac{\partial u}{\partial x} - \eta_1 \theta, \tag{53}$$

$$\frac{\partial^2 u}{\partial t^2} = \frac{\partial^2 u}{\partial x^2} - \eta_1 \frac{\partial \theta}{\partial x} - \epsilon \frac{\partial u}{\partial t}, \tag{54}$$

$$\frac{\partial^2 \theta}{\partial x^2} = \left(1 + \sum_{n=1}^{N} \frac{\tau_0^n}{n!} \frac{\partial^n}{\partial t^n}\right) \left[\frac{\partial \theta}{\partial t} + \eta_2 \frac{\partial}{\partial t}\left(\frac{\partial u}{\partial x}\right) - Q\right], \tag{55}$$

or after using Laplace transform

$$\bar{\tau} = \bar{\sigma} = \frac{\mathrm{d}\bar{u}}{\mathrm{d}x} - \eta_1 \bar{\theta}, \tag{56}$$

$$\left(\frac{\mathrm{d}^2}{\mathrm{d}x^2} - \eta_7\right) \bar{u} - \eta_1 \frac{\mathrm{d}\bar{\theta}}{\mathrm{d}x} = 0, \tag{57}$$

$$\left(\frac{\mathrm{d}^2}{\mathrm{d}x^2} - \eta_5\right) \bar{\theta} - \eta_6 \frac{\mathrm{d}\bar{u}}{\mathrm{d}x} = -Q_1 \mathrm{e}^{-(s/\vartheta)x}, \tag{58}$$

where

$$\eta_7 = s(\epsilon + s). \tag{59}$$

Elimination $\bar{\theta}$ or $\bar{u}$ from Equations (54) and (55), one obtains:

$$\left(\frac{\mathrm{d}^4}{\mathrm{d}x^4} - 2c_1 \frac{\mathrm{d}^2}{\mathrm{d}x^2} + c_2\right) \bar{u}(x) = c_3 \mathrm{e}^{-(s/\vartheta)x}, \tag{60}$$

$$\left(\frac{\mathrm{d}^4}{\mathrm{d}x^4} - 2c_1 \frac{\mathrm{d}^2}{\mathrm{d}x^2} + c_2\right) \bar{\theta}(x) = c_4 \mathrm{e}^{-(s/\vartheta)x}, \tag{61}$$

where the coefficients c_1, c_2, c_3 and c_4 are given by

$$c_1 = \frac{1}{2}(\eta_5 + \eta_7 + \eta_1 \eta_6), \quad c_2 = \eta_5 \eta_7, \quad c_3 = \frac{\eta_1 Q_1 s}{\vartheta}, \quad c_4 = \left(\eta_7 - \frac{s^2}{\vartheta^2}\right) Q_1. \tag{62}$$

The solutions of Equations (60) and (61) can be represented as

$$\bar{u}(x) = \sum_{n=1}^{2} (\mathcal{A}_n \mathrm{e}^{\kappa_n x} + \mathcal{B}_n \mathrm{e}^{-\kappa_n x}) + \bar{c}_3 \mathrm{e}^{-\kappa_3 x}, \tag{63}$$

$$\bar{\theta}(x) = \sum_{n=1}^{2} \alpha_n (\mathcal{A}_n \mathrm{e}^{\kappa_n x} - \mathcal{B}_n \mathrm{e}^{-\kappa_n x}) - \alpha_3 \bar{c}_3 \mathrm{e}^{-\kappa_3 x}, \tag{64}$$

where $\mathcal{A}_n$ and $\mathcal{B}_n$, $(n = 1,2)$ are two integral constants subject to s to be obtained by the boundary conditions, while α_j and $\bar{c}_3$ are represented as

$$\alpha_j = \frac{\kappa_j^2 - \eta_7}{\kappa_j \eta_1}, \quad \bar{c}_3 = \frac{c_3}{\kappa_3^4 - 2c_1 \kappa_3^2 + c_2}, \quad \kappa_3 = \frac{s}{\vartheta}, \quad j = 1,2,3. \tag{65}$$

In Equations (63) and (64), κ_1 and κ_2 are the roots of the individual equation

$$\kappa^4 - 2c_1 \kappa^2 + c_2 = 0, \tag{66}$$

and they are provided by

$$\kappa_1^2, \kappa_2^2 = c_1 \mp \sqrt{c_1^2 - c_2}. \tag{67}$$

The component of stress $\bar{\tau}$ may be calculated using Equations (63) and (64) in Equation (56) as

$$\bar{\tau} = \bar{\sigma} = \sum_{n=1}^{2} \bar{\alpha}_n (\mathcal{A}_n \mathrm{e}^{\kappa_n x} - \mathcal{B}_n \mathrm{e}^{-\kappa_n x}) - \bar{\alpha}_3 \bar{c}_3 \mathrm{e}^{-\kappa_3 x}, \tag{68}$$

where

$$\bar{\alpha}_j = \kappa_j - \alpha_j \eta_1, \quad j = 1,2,3. \tag{69}$$

Once again, one can easily get the unknown parameters $\mathcal{A}_n$, $\mathcal{B}_n$ in the form

$$\mathcal{A}_1 = \frac{\bar{c}_3(\alpha_2\kappa_2-\alpha_3\kappa_3)(\mathrm{e}^{-\kappa_1}-\mathrm{e}^{-\kappa_3})}{(\alpha_2\kappa_2-\alpha_1\kappa_1)(\mathrm{e}^{\kappa_1}-\mathrm{e}^{-\kappa_1})},\quad \mathcal{B}_1 = -\frac{\bar{c}_3(\alpha_2\kappa_2-\alpha_3\kappa_3)(\mathrm{e}^{\kappa_1}-\mathrm{e}^{-\kappa_3})}{(\alpha_2\kappa_2-\alpha_1\kappa_1)(\mathrm{e}^{\kappa_1}-\mathrm{e}^{-\kappa_1})},$$
$$\mathcal{A}_2 = \frac{\bar{c}_3(\alpha_1\kappa_1-\alpha_3\kappa_3)(\mathrm{e}^{-\kappa_2}-\mathrm{e}^{-\kappa_3})}{(\alpha_1\kappa_1-\alpha_2\kappa_2)(\mathrm{e}^{\kappa_2}-\mathrm{e}^{-\kappa_2})},\quad \mathcal{B}_2 = -\frac{\bar{c}_3(\alpha_1\kappa_1-\alpha_3\kappa_3)(\mathrm{e}^{\kappa_2}-\mathrm{e}^{-\kappa_3})}{(\alpha_1\kappa_1-\alpha_2\kappa_2)(\mathrm{e}^{\kappa_2}-\mathrm{e}^{-\kappa_2})}. \tag{70}$$

7. Numerical Results and Validations

This section shows numerical findings that examine the impact of several parameters on the thermoelastic response of the thin, slim strip. For numerical computations, the material of the thin slim strip is identified as copper. The fundamental material parameters that must be specified are provided [26].

$$K = 386\ (\mathrm{W\,m^{-1}K^{-1}}),\quad \lambda = 7.76\times10^{10}\ (\mathrm{N\,m^{-2}}),\quad \mu = 3.86\times10^{10}\ (\mathrm{N\,m^{-2}}),$$
$$\rho = 8954\ (\mathrm{Kg\,m^{-3}}),\quad T_0 = 293\ (\mathrm{K}),\quad c_v = 383.1\ (\mathrm{J\,kg^{-1}\,K^{-1}}),\quad \alpha_t = 1.78\times10^{-5}(\mathrm{K^{-1}}).$$

In all figures, the following values are fixed (except otherwise stated), $\vartheta = 2$, $\xi = 0.1$, $t = 0.5$. The dimensionless length of the thin slim strip is $L = 0.8$. The relaxation time of the simple and refined LS theories is fixed as $t_0 = 0.02$ and $Q_0 = 10$. We return to the old situation (local theory of elasticity) as the nonlocal parameter is vanishing ($\xi = 0$). In Equation (25), ϵ is referred to as the magneto thermoelasticity parameter since it is given in terms of the magnetic field intensity H_x, the magnetic permeability μ_0, and the electric conductivity σ_0. It may take values ranging from 0 to 10. The value $\epsilon = 0$ represents the case without a magnetic field.

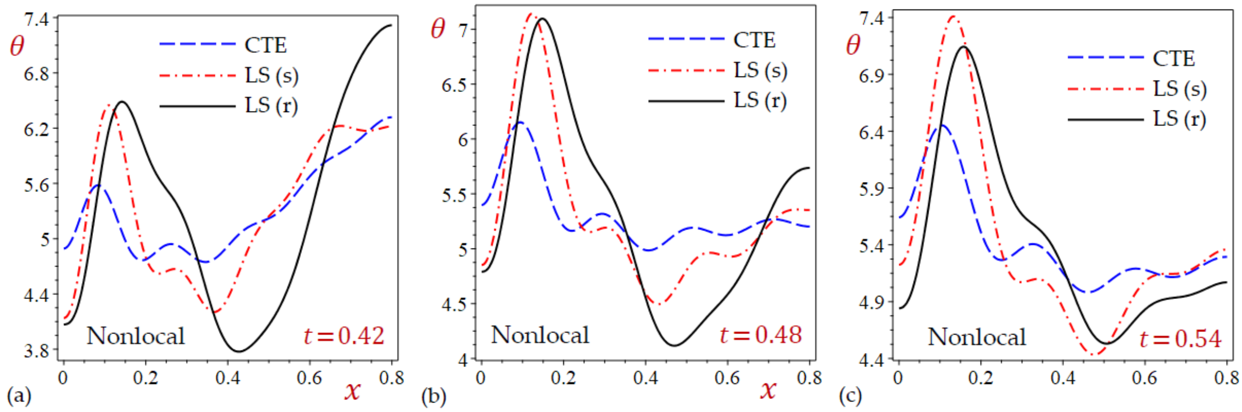

Fig 1. Nonlocal temperature θ distributions of the slim strip for different times t according to all theories.

In what follows we will describe and compare the analytical outcomes found in the previous sections via some numerical examples which demonstrate the distributions of temperature θ ($\equiv \theta^*$), displacement u ($\equiv 10^3u^*$), dilatation e ($\equiv 10^3e^*$), and different stresses σ ($\equiv 10^2\sigma^*$) and τ ($\equiv 10^2\tau^*$). The results due to the classical theory with the simple and refined generalized LS theories are illustrated. In addition, all variables will be presented in both nonlocal and local cases.

7.1 Effect of the Time Instant

In this case, some examples are introduced to show the influence of time instant t on the field variables for fixed values of the moving heat source velocity $\vartheta = 2$, magneto thermoelasticity parameter $\epsilon = 5$, and the nonlocal parameter $\xi = 0.1$. For the comparison of the outcomes, the temperature, displacement, dilatation, and stress of the strip are shown in Figures 1-8.

In Figure 1, the nonlocal distributions of temperature θ of the slim strip for different times t are presented according to all theories. The change in time instance is studied. The temperature θ is very sensitive to the change in t. The amplitudes of the CTE temperature waves are the smallest ones. The amplitude of the temperature wave remains the highest because of the refined theory for $t = 0.42$ and $t = 0.48$ and smaller than the simple theory for $t = 0.54$. It is interesting here to see that the temperatures due to the nonlocal thermoelasticity theory are the same as those due to the local thermoelasticity theory. That is because the nonlocal term has not affected the temperature.

Figure 2 exhibits the nonlocal distributions of displacement u of the slim strip for different times t according to all theories. However, Figure 3 presents the local distributions of displacement u of the slim strip. The local and nonlocal displacements decrease as the dimensionless time increases. Also, the classical theory yields the greatest displacements while the refined theory yields, in most cases, the smallest displacements. It is apparent that the displacements are extremely sensitive to the variation of time, especially, for the local case.

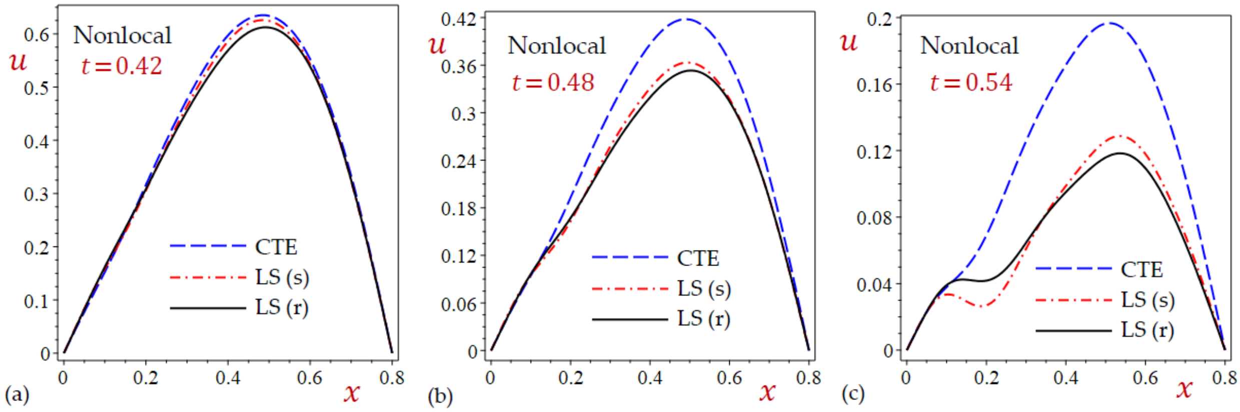

Fig 2. Nonlocal displacement u distributions of the slim strip for different times t according to all theories.

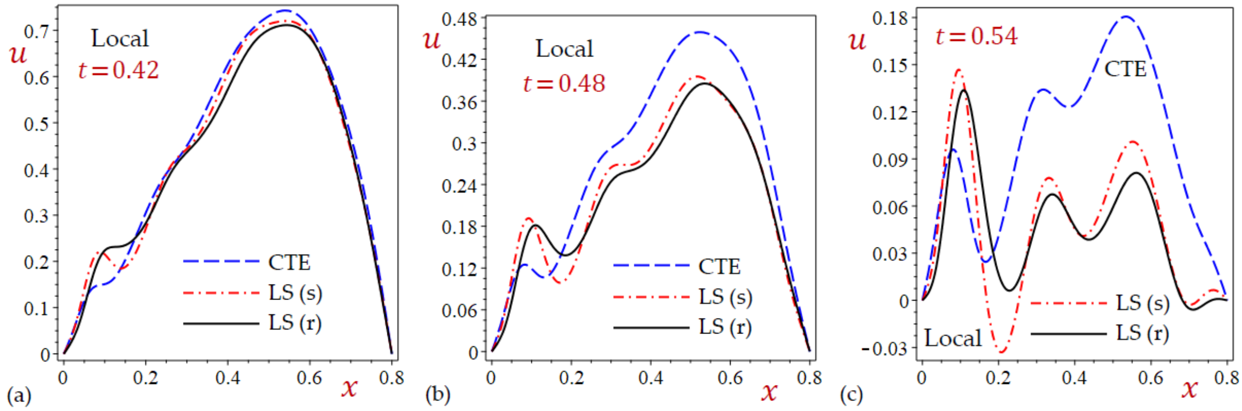

Fig 3. Local displacement u distributions of the slim strip for different times t according to all theories.

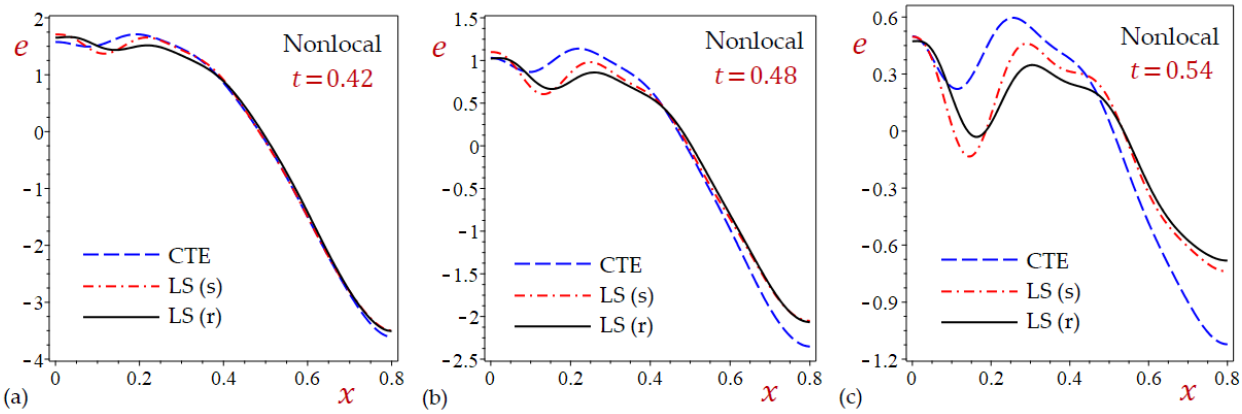

Fig 4. Nonlocal dilatation e distributions of the slim strip for different times t according to all theories.

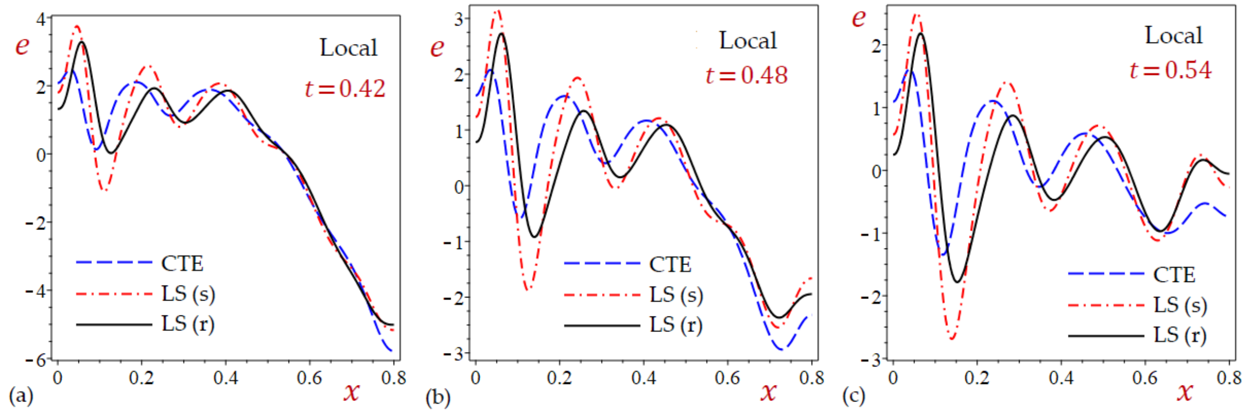

Fig 5. Local dilatation e distributions of the slim strip for different times t according to all theories.

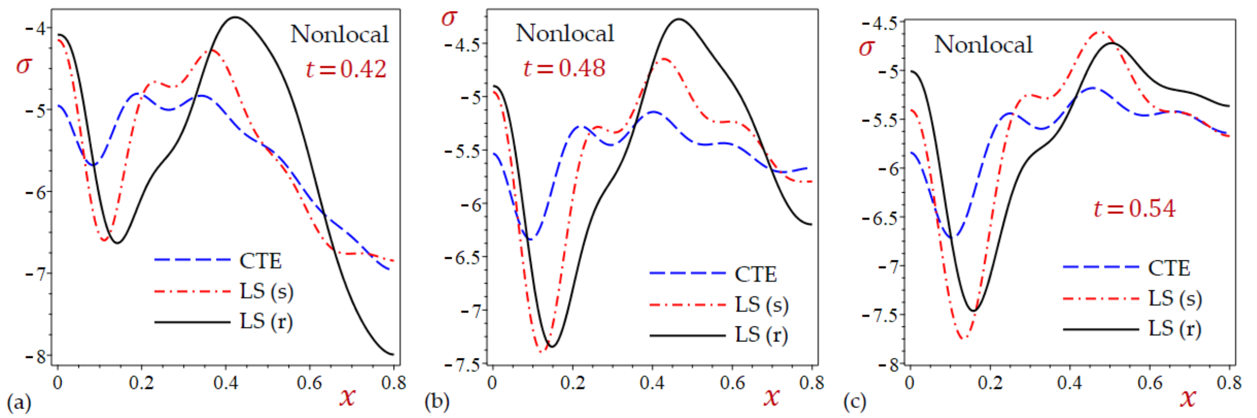

Fig 6. Nonlocal stress σ distributions of the slim strip for different times t according to all theories.

Figures 4 and 5 show the nonlocal and local distributions of dilatation e of the slim strip for different times t according to all theories. Dilatation decreases across the x-axis of the slim strip. Also, the dilatation decreases as t increases. The classical theory yields a dilatation wave with the largest amplitude in the nonlocal case and with the smallest amplitude in the local case.

Figures 6 and 7 show the nonlocal and local distributions of stress σ of the slim strip for different times t according to all theories. The local stress may be similar to the nonlocal one in all cases. In both cases, the stress wave caused by the refined theory has the largest amplitude for $t = 0.42$ and $t = 0.48$. However, the stress wave caused by the simple theory has the largest amplitude for $t = 0.54$.

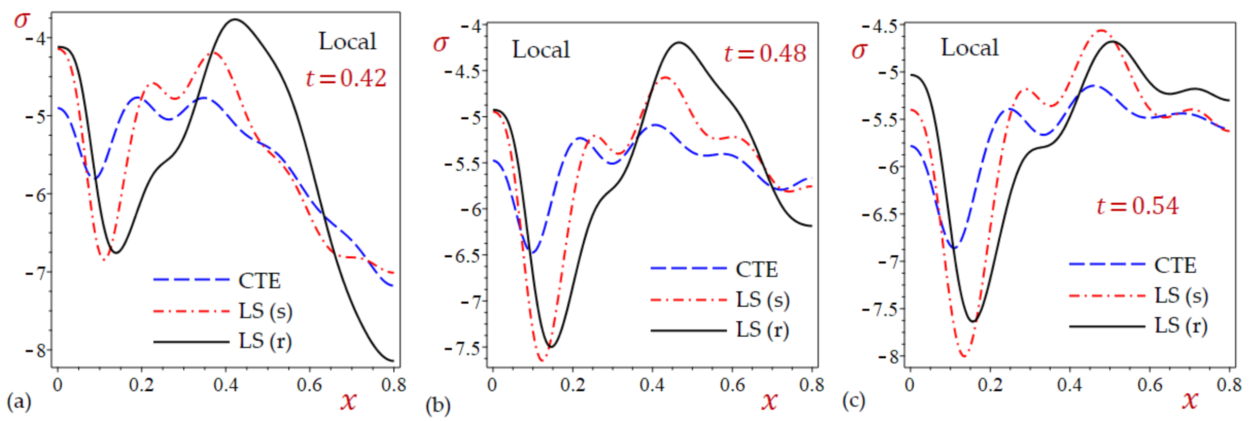

Fig 7. Local stress σ distributions of the slim strip for different times t according to all theories.

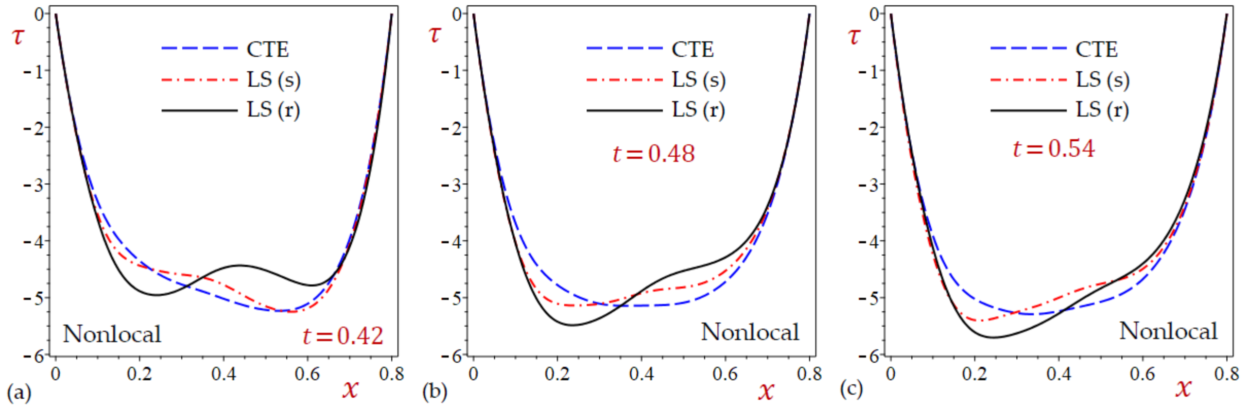

Fig 8. Nonlocal stress τ distributions of the slim strip for different times t according to all theories.

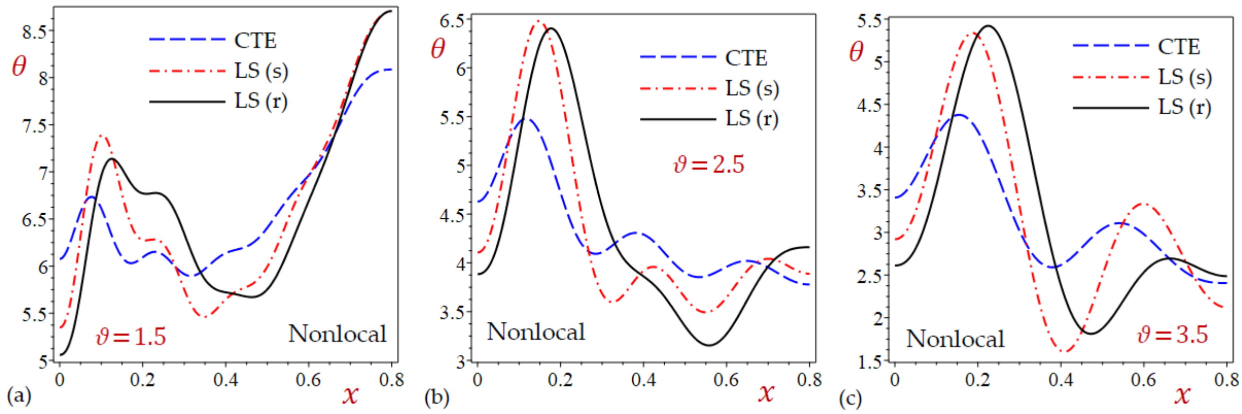

Fig 9. Nonlocal temperature θ distributions of the slim strip for different velocities ϑ according to all theories.

Finally, Figure 8 shows the pure nonlocal stress τ distributions of the slim strip for different times t according to all theories. It is to be mentioned that the pure nonlocal stress τ vanishes at the ends of the slim strip according to the boundary conditions. τ is sensitive to the variation of t.

7.2 Effect of Moving Heat Source Velocity Parameter

The second case considered here is to examine the dimensionless temperature, displacement, dilatation, and stress change with different values of the velocity of the moving source of heat ϑ as the other parameters are considered constant ($t = 0.5$, $\epsilon = 5$, and $\xi = 0.1$). The results for this case are illustrated in Figures 9-15. In this study, we will investigate the assumption that the pattern of changes that occur across all field variables for the velocity parameters of moving heat sources is considerably different.

In Figure 9, the nonlocal distributions of temperature θ of the slim strip for different moving heat source velocities ϑ are presented according to all theories. The change in ϑ is studied, and θ is very sensitive to the variation ϑ. The amplitudes of the CTE temperature waves are the smallest ones. The amplitude of the temperature wave caused by the simple theory is still the largest one in most positions. In general, the temperature θ reduces as the velocity of moving heat source ϑ rises. Once again, it is interesting here to see that the temperatures due to the nonlocal thermoelasticity theory are the same as those due to the local thermoelasticity theory.

Figure 10 shows the nonlocal distributions of displacement u ($\hat{u} = 10u$, $\breve{u} = 100u$) of the slim strip for different moving heat source velocities ϑ according to all theories. However, Figure 11 illustrates the corresponding local distributions of displacement u of the slim strip. The displacement satisfies the boundary conditions at the endpoints of the slim strip and gets some negative values in different positions. The local and nonlocal displacements decrease as the velocity of a moving heat source ϑ rises.

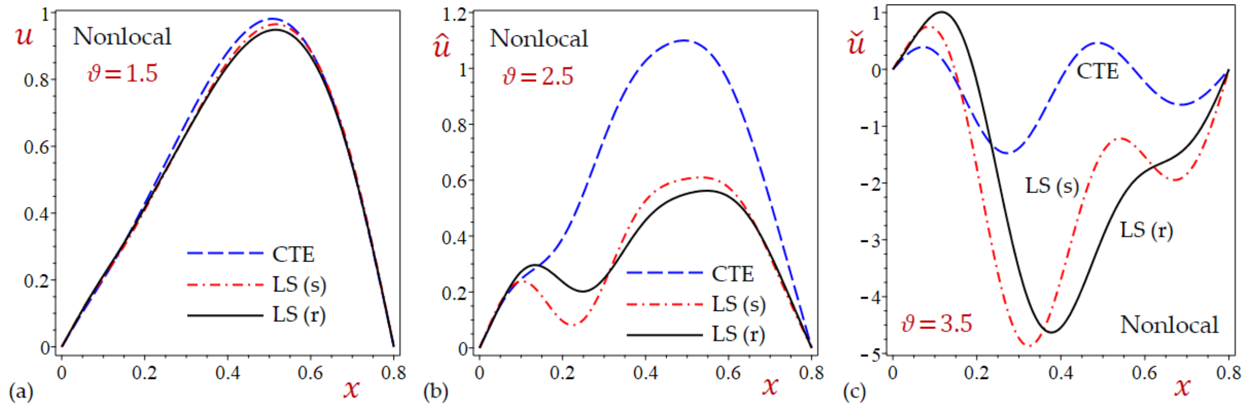

Fig 10. Nonlocal displacement u distributions of the slim strip for different velocities ϑ according to all theories.

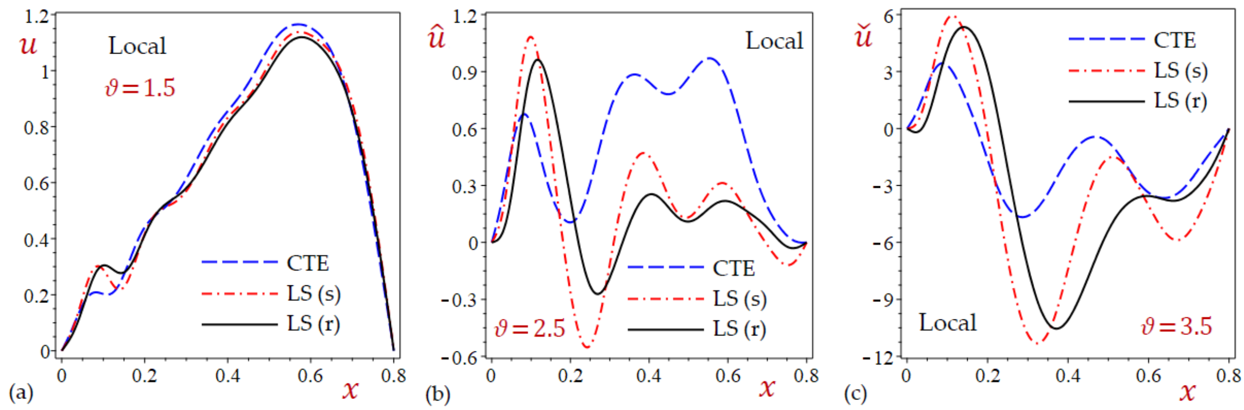

Fig 11. Local displacement u distributions of the slim strip for different velocities ϑ according to all theories.

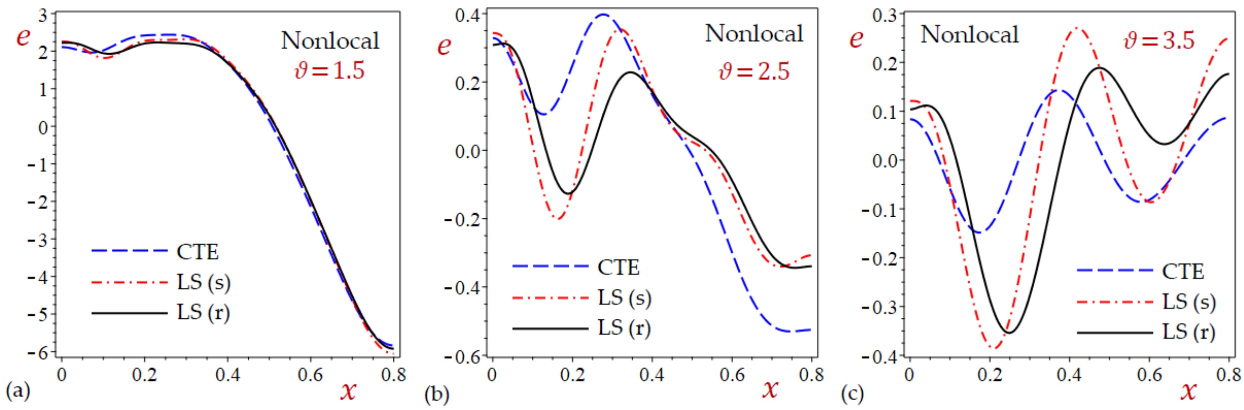

Fig 12. Nonlocal dilatation e distributions of the slim strip for different velocities ϑ according to all theories.

Also, the classical theory yields the greatest displacements while the refined theory yields, in most cases, the smallest displacements. The displacements are extremely sensitive to the change of the moving heat source velocity ϑ, especially in the local case.

Figures 12 and 13 show the nonlocal and local distributions of dilatation e of the slim strip for different moving heat source velocities ϑ according to all theories. The amplitudes of dilatation waves decrease across the x-axis of the slim strip as the moving heat source velocity ϑ rises. The amplitude of the dilatation wave caused by classical theory may be the largest one when $\vartheta = 1.5$ and $\vartheta = 2.5$. However, the amplitude of the dilatation wave caused by the LS (s) theory is the largest one when $\vartheta = 3.5$. The dilatations are more sensitive to the variation of the moving heat source velocity ϑ when the local case is considered.

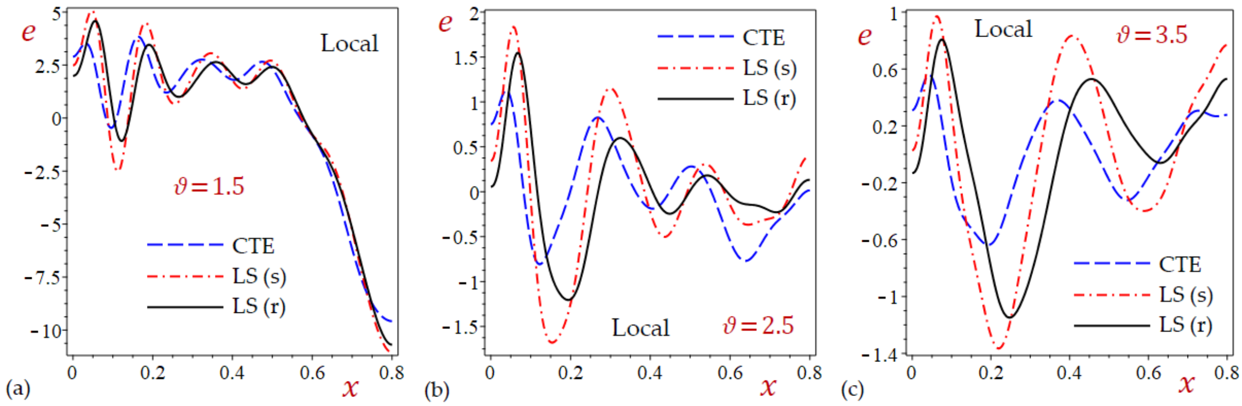

Fig 13. Local dilatation e distributions of the slim strip for different velocities ϑ according to all theories.

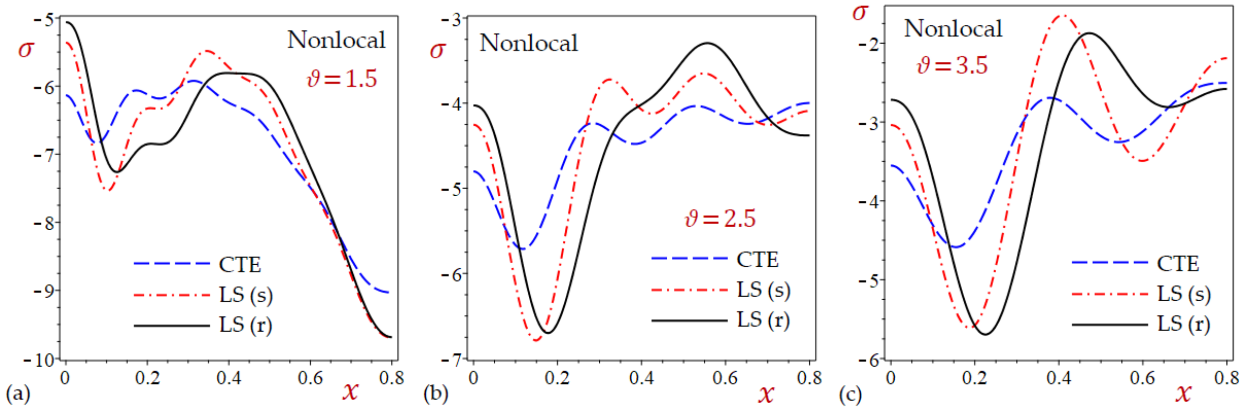

Fig 14. Nonlocal stress σ distributions of the slim strip for different velocities ϑ according to all theories.

Figures 14 and 15 show the nonlocal and local distributions of stress σ of the slim strip for different moving heat source velocities ϑ according to all theories. The local stress may be similar to the nonlocal one in all cases. In both cases, the stress wave is extremely sensitive to the change of the moving heat source velocity ϑ. The stresses decrease with the increase in the moving heat source velocities ϑ.

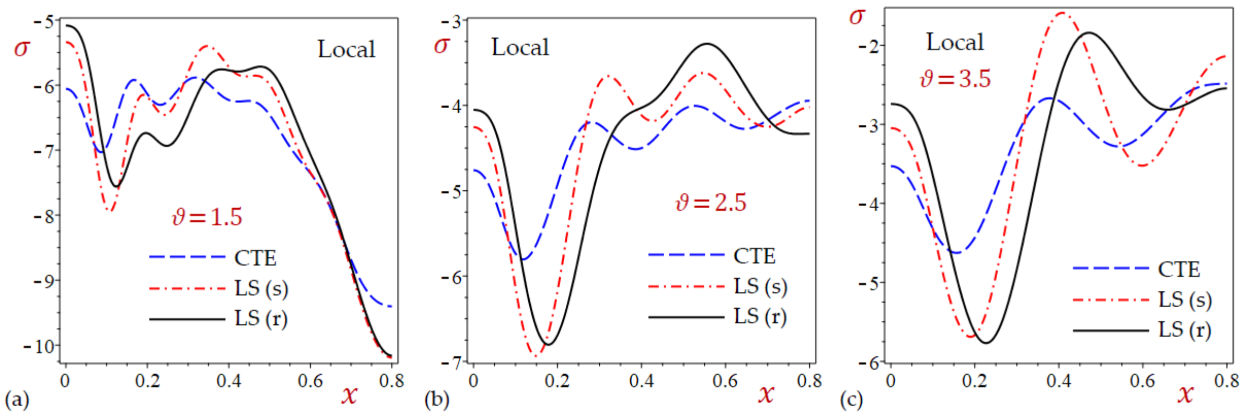

Fig 15. Local stress σ distributions of the slim strip for different velocities ϑ according to all theories.

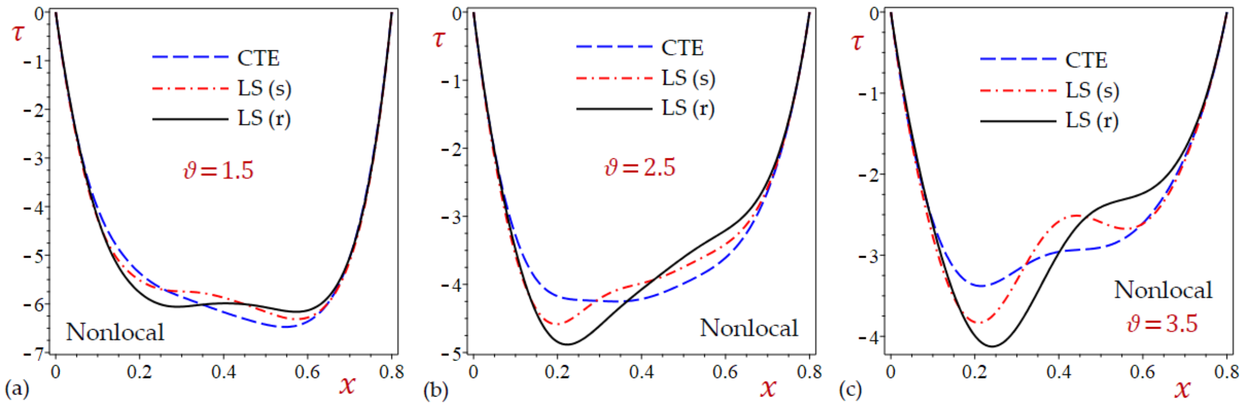

Fig 16. Nonlocal stress τ distributions of the slim strip for different velocities ϑ according to all theories.

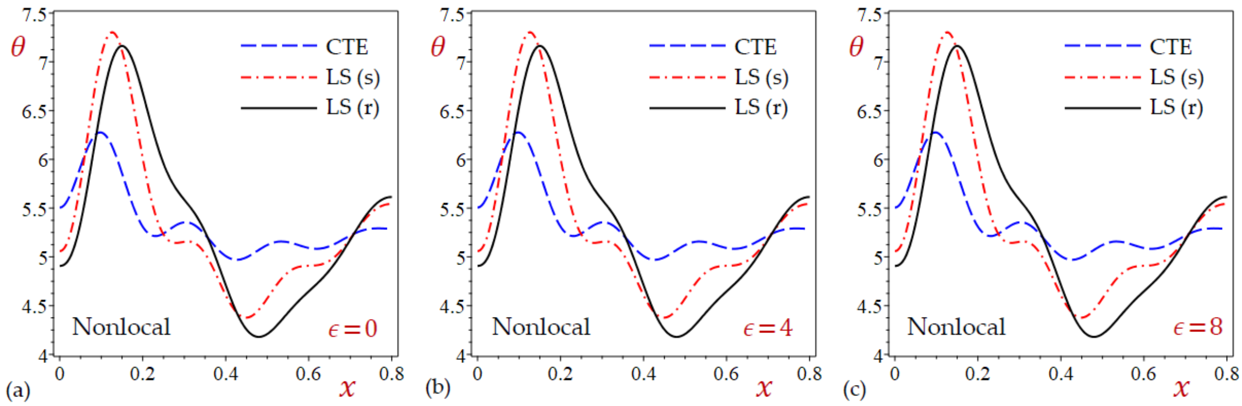

Fig 17. Nonlocal temperature θ distributions of the slim strip for different magneto thermoelastic parameters ϵ according to all theories.

In Figure 16, the pure nonlocal stress τ distributions of the slim strip are presented for different moving heat source velocities ϑ according to all theories. It is to be mentioned that the pure nonlocal stress τ vanishes at the ends of the slim strip according to the boundary conditions. The absolute value of τ decreases as ϑ increases and τ is sensitive to the change of different moving heat source velocities ϑ between the ends of the slim strip.

7.3 Influence of the Applied Magnetic Field

In the last case, we illustrate how the quantities of the field change with the different values of the applied magneto thermoelastic parameter ϵ ($\epsilon = 0,\ 4,\ 8$) with constants $\vartheta = 2$, $t = 0.5$, and $\xi = 0.1$. Results of all variables are obtained and presented graphically in Figs17-24.

Figure 17 exhibits the nonlocal distributions of temperature θ of the slim strip for different magneto thermoelastic parameters ϵ are presented according to all theories. The temperature θ has low sensitivity to the variations magneto thermoelastic parameters ϵ. The amplitudes of the CTE temperature waves are the smallest ones. It is interesting here to see that the temperatures due to the nonlocal thermoelasticity theory are the same as those due to the local thermoelasticity theory.

Figure 18 shows the nonlocal distributions of displacement u of the slim strip for different magneto thermoelastic parameters ϵ according to all theories. However, Figure 19 shows the corresponding local distributions of displacement u of the slim strip. The displacement satisfies the boundary conditions at the endpoints of the slim strip. The displacements are extremely sensitive to the variation in the magneto thermoelastic parameters ϵ, mainly for the local case. The local and nonlocal displacements decrease as the magneto thermoelastic parameter ϵ increases. Also, the classical theory yields the greatest displacements while the refined theory yields, in most cases, the smallest displacements.

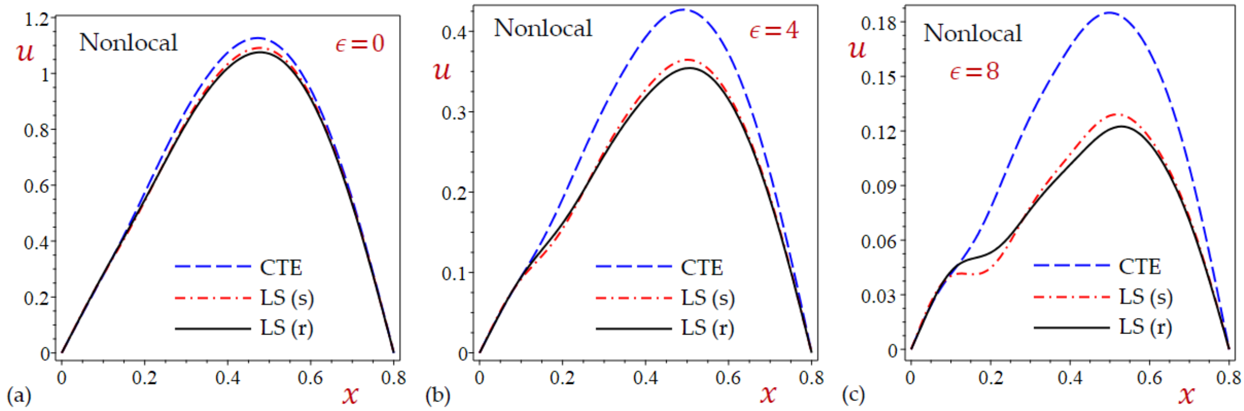

Fig 18. Nonlocal displacement u distributions of the slim strip for different magneto thermoelastic parameters ϵ according to all theories.

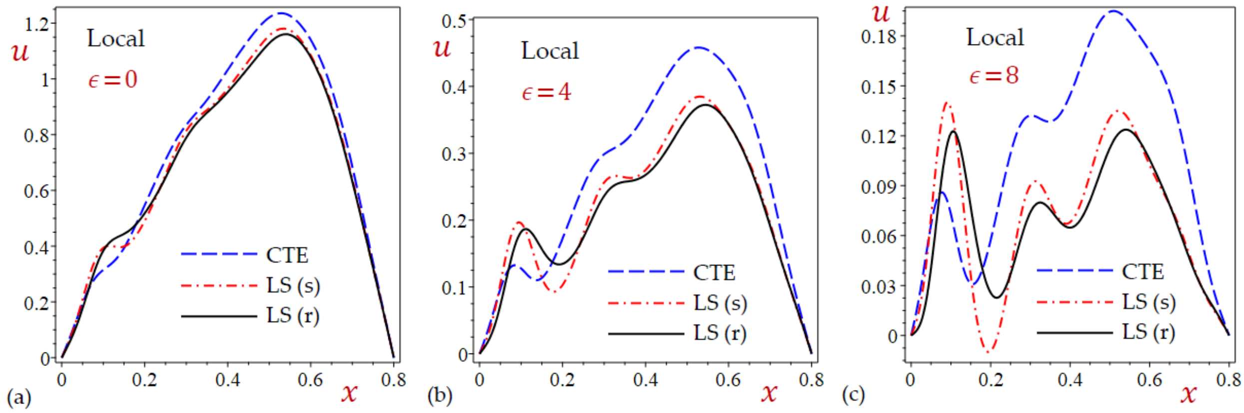

Fig 19. Local displacement u distributions of the slim strip for different magneto thermoelastic parameters ϵ according to all theories.

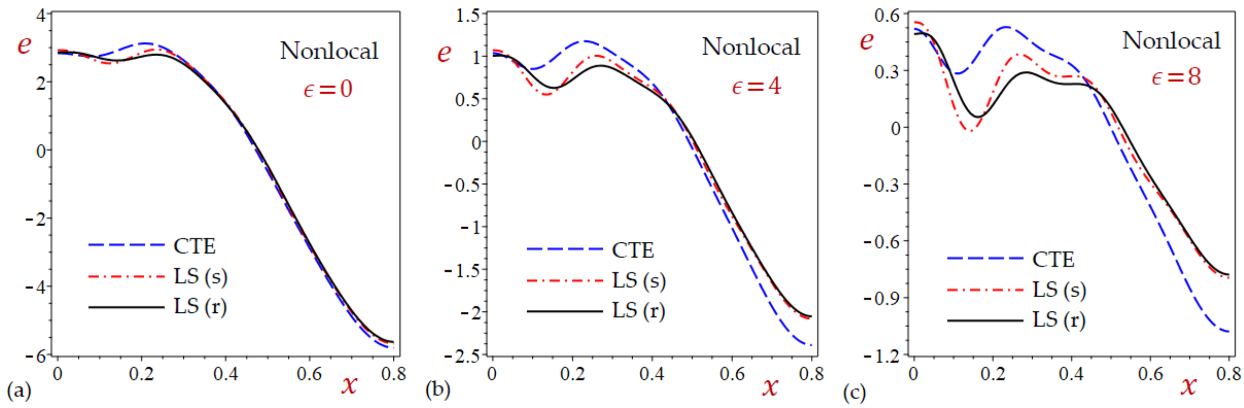

Fig 20. Nonlocal dilatation e distributions of the slim strip for different magneto thermoelastic parameters ϵ according to all theories.

Figure 20 shows the nonlocal distributions of dilatation e of the slim strip for different magneto thermoelastic parameters ϵ according to all theories. However, Figure 21 shows the corresponding local distributions of dilatation e of the slim strip. The dilatations are very sensitive to the variation in the magneto thermoelastic parameters ϵ, mainly for the local case. The local and nonlocal dilatations decrease as the magneto thermoelastic parameter ϵ increases. The amplitudes of dilatation waves decrease along the x-axis of the slim strip as the magneto thermoelastic parameter ϵ increases. The amplitude of the dilatation wave caused by classical theory may be the largest one in the nonlocal case and the smallest one in the local case.

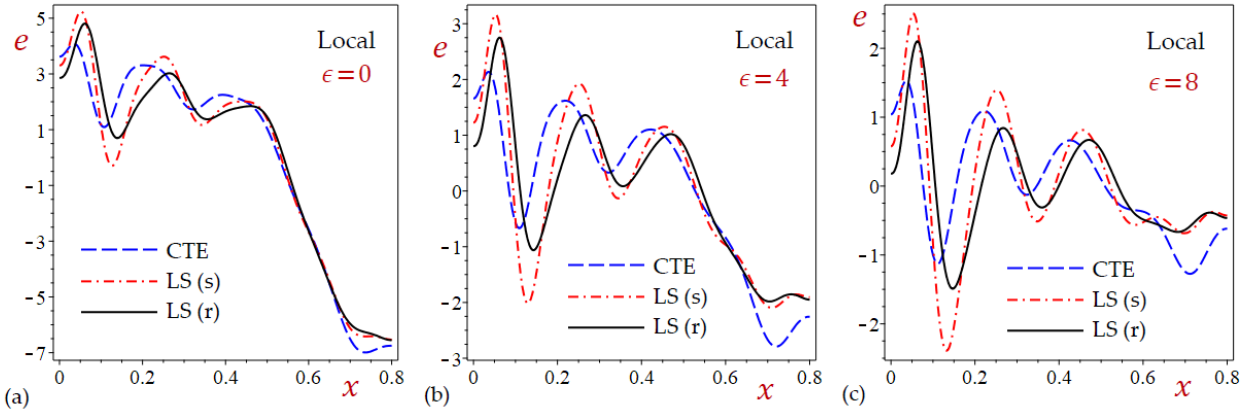

Fig 21. Local dilatation e distributions of the slim strip for different magneto thermoelastic parameters ϵ according to all theories.

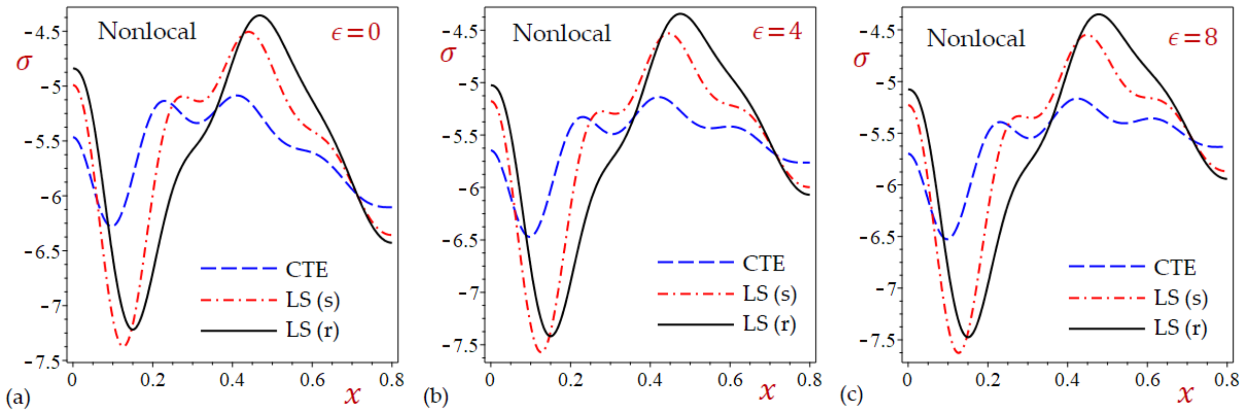

Fig 22. Nonlocal stress σ distributions of the slim strip for different magneto thermoelastic parameters ϵ according to all theories.

Figures 22 and 23 show the nonlocal and local distributions of stress σ of the slim strip for different magneto thermoelastic parameters ϵ according to all theories. The local stress may be similar to the nonlocal one in all cases. In both cases, the stress wave is extremely sensitive to the change of the magneto thermoelastic parameter ϵ. The stresses have very slow variation with the change in magneto thermoelastic parameters ϵ.

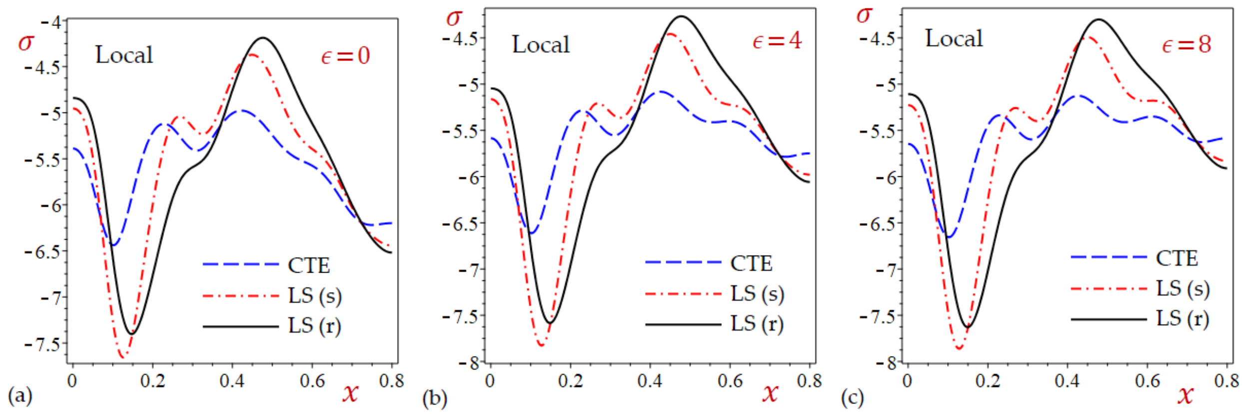

Fig 23. Local stress σ distributions of the slim strip for different magneto thermoelastic parameters ϵ according to all theories.

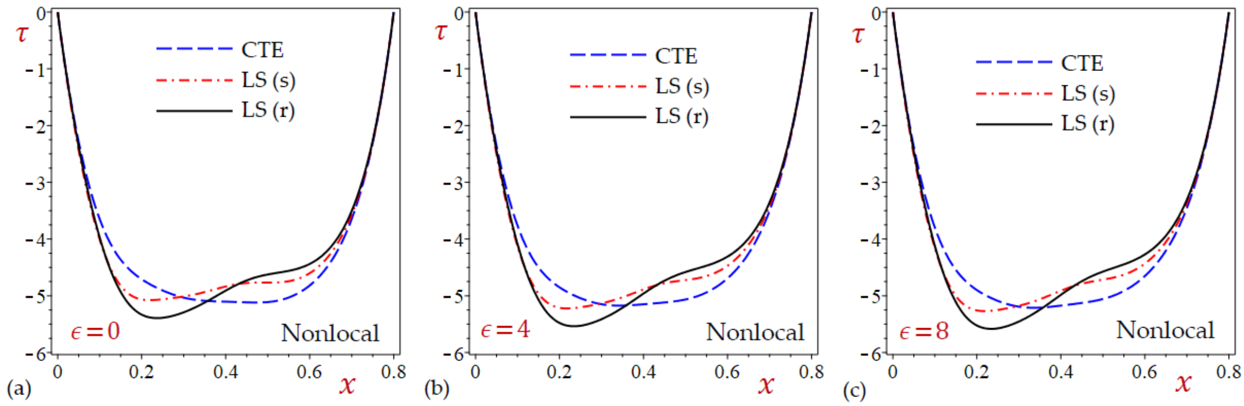

Fig 24. Nonlocal stress τ distributions of the slim strip for different magneto thermoelastic parameters ϵ according to all theories.

Figure 24 shows the pure nonlocal stress τ distributions of the slim strip for different magneto thermoelastic parameters ϵ according to all theories. The pure nonlocal stress τ vanishes at the ends of the slim strip according to the boundary conditions. The nonlocal stress τ has low sensitivity to the variations of magneto thermoelastic parameters ϵ.

8. Conclusions

In this work, the dynamic effect of an isotropic thin slim strip exposed to a magnetic field and moving heat source based on the nonlocal thermoelasticity theory is investigated. The solution is obtained with the aid of Laplace's transformation method and its inversion. The effect of nonlocal parameters, moving heat source velocity, and exposed magnetic field on the transient responses of the thin slim strip is discussed. Based on the numerical findings, the following deductions can be drawn:

- The nonlocal parameter ξ has major effects on displacement, dilatation, and nonlocal stress fields, however, it has little effect on the temperature and thermal stress. The temperature may remain unchanged with the changes in the nonlocal parameter.
- The finite speed propagation phenomenon is shown in all figures by comparing the classical thermoelasticity theory with the generalized (simple and refined) Lord and Sulmann theory.
- The influence of the applied magnetic field ϵ on the studied quantities is very significant.
- The value of moving heat source velocity ϑ has a fundamental part in changing the value of the physical quantities distribution. It has a huge impact on displacement, dilatation, temperature, and distributions of local and nonlocal stress.
- The dimensionless time parameter t causes significant changes in all the studied quantities.

Acknowledgments

The authors (Hafed and Zenkour) extend their appreciation to the Deanship of Research and Graduate Studies at King Khalid University for funding this work through Large Research Project under grant number RGP2/80/45.

References

[1] A. C. Eringen, Nonlocal polar elastic continua, *International Journal of Engineering Science*, Vol. 10, pp. 1-16, 1972.

[2] A. C. Eringen, On differential equations of nonlocal elasticity and solutions of screw dislocation and surface waves, *Journal of Applied Physics*, Vol. 54, pp. 4703-4710, 1983.

[3] A. C. Eringen, D. Edelen, On nonlocal elasticity, *International Journal of Engineering Science*, Vol. 10, pp. 233-248, 1972.

[4] A. E. Abouelregal, B. O. Mohamed, Fractional order thermoelasticity for a functionally graded thermoelastic nanobeam induced by a sinusoidal pulse heating, *Journal of Computational and Theoretical Nanoscience*, Vol. 15, pp. 1233-1242, 2018.

[5] A. E. Abouelregal, A. M. Zenkour, Thermoelastic response of nanobeam resonators subjected to exponential decaying time varying load, *Journal of Theoretical and Applied Mechanics*, Vol. 55, pp. 937-948, 2017.

[6] A. E. Abouelregal, A. M. Zenkour, Nonlocal thermoelastic model for temperature-dependent thermal conductivity nanobeams due to dynamic varying loads, *Microsystem Technologies*, Vol. 24, pp. 1189-1199, 2018.

[7] J. Afzali, Z. Alemipour, M. Hesam, High resolution image with multi-wall carbon nanotube atomic force microscopy tip (research note), *International Journal of Engineering*, Vol. 26, pp. 671-676, 2013.

[8] J. W. R. S. Dhaliwal, Uniqueness in generalized nonlocal thermoelasticity, *Journal of Thermal Stresses*, Vol. 16, pp. 71-77, 1993.

[9] E. Inan, A. Eringen, Nonlocal theory of wave propagation in thermoelastic plates, *International Journal of Engineering Science*, Vol. 29, pp. 831-843, 1991.

[10] Z. Khisaeva, M. Ostoja-Starzewski, Thermoelastic damping in nanomechanical resonators with finite wave speeds, *Journal of Thermal Stresses*, Vol. 29, pp. 201-216, 2006.

[11] C. C. Koutsoumaris, K. Eptaimeros, G. Tsamasphyros, A different approach to Eringen's nonlocal integral stress model with applications for beams, *International Journal of Solids and Structures*, Vol. 112, pp. 222-238, 2017.

[12] K. Liew, Y. Zhang, L. Zhang, Nonlocal elasticity theory for graphene modeling and simulation: prospects and challenges, *Journal of Modeling in Mechanics and Materials*, Vol. 1, pp., 2017.

[13] H. W. Lord, Y. Shulman, A generalized dynamical theory of thermoelasticity, *Journal of the Mechanics and Physics of Solids*, Vol. 15, pp. 299-309, 1967.

[14] K. Rajneesh, M. Aseem, R. Rekha, Transient analysis of nonolocal microstretch thermoelastic thick circular plate with phase lags, *Mediterranean Journal of Modeling and Simulation*, Vol. 9, pp. 025-042, 2018.

[15] P. Ribeiro, Non-local effects on the non-linear modes of vibration of carbon nanotubes under electrostatic actuation, *International Journal of Non-Linear Mechanics*, Vol. 87, pp. 1-20, 2016.

[16] A. Zenkour, A. Abouelregal, Magnetothermoelastic Interaction in a Rod of Finite Length Subjected to Moving Heat Sources Via Eringen's Nonlocal Model, *Journal of Engineering Physics and Thermophysics*, Vol. 95, pp. 651-661, 2022.

[17] A. M. Zenkour, A. E. Abouelregal, Nonlocal thermoelastic vibrations for variable thermal conductivity nanobeams due to harmonically varying heat, *Journal of Vibroengineering*, Vol. 16, pp. 3665-3678, 2014.

[18] A. M. Zenkour, A. E. Abouelregal, Nonlocal thermoelastic nanobeam subjected to a sinusoidal pulse heating and temperature-dependent physical properties, *Microsystem Technologies*, Vol. 21, pp. 1767-1776, 2015.

[19] A. M. Zenkour, A. E. Abouelregal, Nonlinear effects of thermo-sensitive nanobeams via a nonlocal thermoelasticity model with relaxation time, *Microsystem Technologies*, Vol. 22, pp. 2407-2415, 2016.

[20] N. Sarkar, Thermoelastic responses of a finite rod due to nonlocal heat conduction, *Acta Mechanica*, Vol. 231, pp. 947-955, 2020.

[21] E. Zarezadeh, V. Hosseini, A. Hadi, Torsional vibration of functionally graded nano-rod under magnetic field supported by a generalized torsional foundation based on nonlocal elasticity theory, *Mechanics Based Design of Structures and Machines*, Vol. 48, pp. 480-495, 2020.

[22] S. Mondal, Memory response for thermal distributions moving over a magneto-thermoelastic rod under Eringen's nonlocal theory, *Journal of Thermal Stresses*, Vol. 43, pp. 72-89, 2020.

[23] F. S. Bayones, S. Mondal, S. M. Abo-Dahab, A. A. Kilany, Effect of moving heat source on a magneto-thermoelastic rod in the context of Eringen's nonlocal theory under three-phase lag with a memory dependent derivative, *Mechanics Based Design of Structures and Machines*, Vol. 51, pp. 2501-2516, 2023.

[24] A. E. Abouelregal, Thermomagnetic behavior of a nonlocal finite elastic rod heated by a moving heat source via a fractional derivative heat equation with a non-singular kernel, *Waves in Random and Complex Media*, Vol. 5, pp. 3056-3076, 2024.

[25] N. Satish, S. Gunabal, K. B. Raju, S. Narendar, Thermoelastic damping in nonlocal rod using three-phase lag heat conduction model, *Journal of Thermal Stresses*, Vol. 44, pp. 955-969, 2021.

[26] T. He, L. Cao, A problem of generalized magneto-thermoelastic thin slim strip subjected to a moving heat source, *Mathematical and Computer Modelling*, Vol. 49, pp. 1710-1720, 2009.

[27] I. A. Abbas, The effects of relaxation times and a moving heat source on a two-temperature generalized thermoelastic thin slim strip, *Canadian Journal of Physics*, Vol. 93, pp. 585-590, 2015.

[28] C. Li, H. Guo, X. Tian, Soret effect on the shock responses of generalized diffusion-thermoelasticity, *Journal of Thermal Stresses*, Vol. 40, pp. 1563-1574, 2017.

[29] S. M. Abo-Dahab, A. E. Abouelregal, M. Marin, Generalized thermoelastic functionally graded on a thin slim strip non-Gaussian laser beam, *Symmetry*, Vol. 12, pp. 1094, 2020.

[30] M. H. Aljadani, A. M. Zenkour, Effect of hydrostatic initial stress on a rotating half-space in the context of a two-relaxation power-law model, *Mathematics*, Vol. 10, pp. 4727, 2022.

[31] M. H. Aljadani, A. M. Zenkour, A Modified Two-Relaxation Thermoelastic Model for a Thermal Shock of Rotating Infinite Medium, *Materials*, Vol. 15, pp. 9056, 2022.

[32] M. A. Kutbi, A. M. Zenkour, Thermomechanical waves in an axisymmetric rotating disk using refined Green–Naghdi models, *International Journal of Applied Mechanics*, Vol. 13, pp. 2150035, 2021.

[33] M. A. Kutbi, A. M. Zenkour, Thermoelastic interactions in an unbounded solid due to a continuous heat source using the modified TPL G–N model, *Waves in Random and Complex Media*, Vol. 32, pp. 1363-1384, 2022.

[34] A. M. Zenkour, Wave propagation of a gravitated piezo-thermoelastic half-space via a refined multi-phase-lags theory, *Mechanics of Advanced Materials and Structures*, Vol. 27, pp. 1923-1934, 2020.

[35] A. M. Zenkour, On generalized three-phase-lag models in photo-thermoelasticity, *International Journal of Applied Mechanics*, Vol. 14, pp. 2250005, 2022.

[36] M. A. Kutbi, A. M. Zenkour, Modified couple stress model for thermoelastic microbeams due to temperature pulse heating, Journal of Computational Applied Mechanics, Vol. 53, pp. 83-101, 2022.

[37] M. Sobhy, A. M. Zenkour, Refined Lord–Shulman theory for 1D response of skin tissue under ramp-type heat, *Materials*, Vol. 15, pp. 6292, 2022.

[38] M. A. Biot, Thermoelasticity and irreversible thermodynamics, *Journal of Applied Physics*, Vol. 27, pp. 240-253, 1956.

[39] G. Honig, U. Hirdes, A method for the numerical inversion of Laplace transforms, *Journal of Computational and Applied Mathematics*, Vol. 10, pp. 113-132, 1984.